Egyptian Journal of Geology

https://egjg.journals.ekb.eg

Geochemical characterizations and rare metal exploration of post-orogenic and anorogenic A-type granites from Gabal El Dob area, Eastern Desert, Egypt

Amr Abdel Aty Abdel Hamid
Nuclear Materials Authority, P.O. 530 El-Maadi, Kattamyia, Egypt

THE orogenic older granitoids of Gabal El Dob area were intruded by post-tectonic younger granitoids, which predominated by alkali feldspar granite and alkali riebeckite granite. These granites occur as two separated and elongated bodies emplaced along a shear zone trending NNE. They are discriminated according to their petrographical studies into subsolvus and hypersolvus granites. Both granitic types consist essentially of perthites and quartz with little amount of plagioclase. The accessory assemblages along the two granitic phases are differing in their quantity and constituents. The hypersolvus granite contains arfvedsonite and riebeckite, which dominantly enclose variable amount of zircon and allanite. Overall, the studied granites are silica and alkali-rich with low contents of MgO, CaO and TiO_2. Comparative geochemical studies indicated that the hypersolvus granite is enriched in total alkalis, Ga, Zr, Nb, Y and ΣREE relative to subsolvus granite. The two granitic phases display REE patterns, characterized by moderately fractionated LREE and nearly flat HREE with a moderate negative Eu anomaly. The subsolvus granite has transitional characteristics between A-type and fractionated I-type granites, but the hypersolvus granite has the most characteristics of A-type granites. The high concentrations of ΣREE in the hypersolus granite (av. 530ppm) are interpreted to the high abundance of REE-bearing allanite. The high contents of ΣREE and Zr in the hypersolvus granite along with the elevated background values of U and Th in both granitic phases could be used as an indicator for rare-metal exploration in Gabal El Dob area.

Keywords: Alkali granite, Anorogenic, REE mineralization, Allanite.

1. Introduction

The younger granitoids of the Eastern Desert of Egypt can be classified as post-orogenic to anorogenic A-type granitoids (Hassanen and Harraz, 1996; Moghazi, 1999; El-Sayed et al., 2001), post-dating the emplacement of I-type calc-alkaline granitoids. They were emplaced during the post-collision and anorogenic stages (e.g. Farahat et al., 2007; Moussa et al., 2008). The ages of the post- to anorogenic (younger) granitoids were formed between 600 and 475 Ma (Rogers et al., 1978; Bentor, 1985).The anorogenic granitoids are alkaline A-type granitoids of dominantly peralkaline to mild aluminous nature, ranging in composition between alkali feldspar granite to syenite. They were emplaced in anorogenic extensional within plate settings (Harris 1982; Katzir et al., 2007). Isochron Rb–Sr ages of alkali granites from the Eastern Desert are obtained with ages of 474-483 Ma (Hashad, 1980; Abdel-Rahman and Martin, 1990).

Intrusions of A-type granites are usually associated with rare metal enrichment, notably U, Th, Zr, Nb and REE. Such enrichment is interpreted in many investigations to arise from extreme differentiation (e.g. Xie et al. 2006), and/or remobilization and concentration of these element by hydrothermal activity (e.g. Marks et al., 2003). In this respect, small intrusive bodies of A-type granitic rocks from Gabal El Dob area, northern Eastern Desert of Egypt, were selected in this study. This region has been previously investigated by Abdel Rahman (2006), Shahin (2015), Hammed et al. (2020), and El-Naggar et al. (2022). The purpose of this paper is to investigate the geochemical characterizations of these granites to clarify their petrogenesis. Particular emphasis is placed on the mineralogy and geochemistry of the rare metals such as REE, Zr, U and Th. The aim of this study is to investigate the A-type granites in Gabal El Dob area for potential to carry rare metal mineralization.

*Corresponding author e-mail: amr_ahamid@yahoo.com
Received: 03/06/2023; Accepted: 01/08/2023
DOI: 10.21608/EGJG.2023.214914.1050

2. Geological setting

Gabal El Dob area is situated in the southern parts of the northern Eastern Desert, northwest of the Safaga city. It can be reached through the highway connecting Safaga on the Red Sea to Sohag on the Nile valley (Fig. 1a).The investigated area is delineated by longitudes 33°21'32"E, 33°24'42"E and latitudes 26°42'38"N, 26°45'46"N, covering an area of ~30Km^2. The Precambrian rocks of Gabal El Dob (Fig. 1b) are characterized by abundant granitic intrusions represented by older and younger granites. The older granites cover the eastern parts of the mapped area and forming the western margins of the Barud syntectonic gneissic tonalite-granodiorite. They are found as many individual bodies of variable dimensions. The younger granites occupy the eastern parts of the study area and contain monzogranite, alkali feldspar granite and alkali riebeckite granite. They often forming highly elevated mountains with sharp slopes covered by their debris and that of their intruding dikes. They are usually invaded by numerous dikes of variable compositions and directions. The monzogranite is exposed in the western parts of the study region and extend beyond it. It is commonly forming low to moderate outcrops, characterized by boulder weathering and exfoliation and traversed by numerous dikes of different compositions.

The alkali feldspar and alkali riebeckite granite were emplaced along a fault system, trending NNE, cutting between older granites and monzogranite. The alkali feldspar granites shows moderate to high elevated mountainous ridges (Fig. 2a). It forms irregular dike-like bodies of 0.5-0.8km wide that narrows gradually over a distance of 3km in NNE direction (Fig. 1b). This granite intrudes the older granites along its eastern peripheries and intrudes the monzogranite with sharp contacts at its western margins. It is dissected by numerous fault zones filled with basic dikes. Generally, this type of granite is medium-grained, light pink, leucocratic, hard and massive, however the southern exposures are coarse-grained. It is cut by numerous aplites, quartz veins and pegmatite pockets.

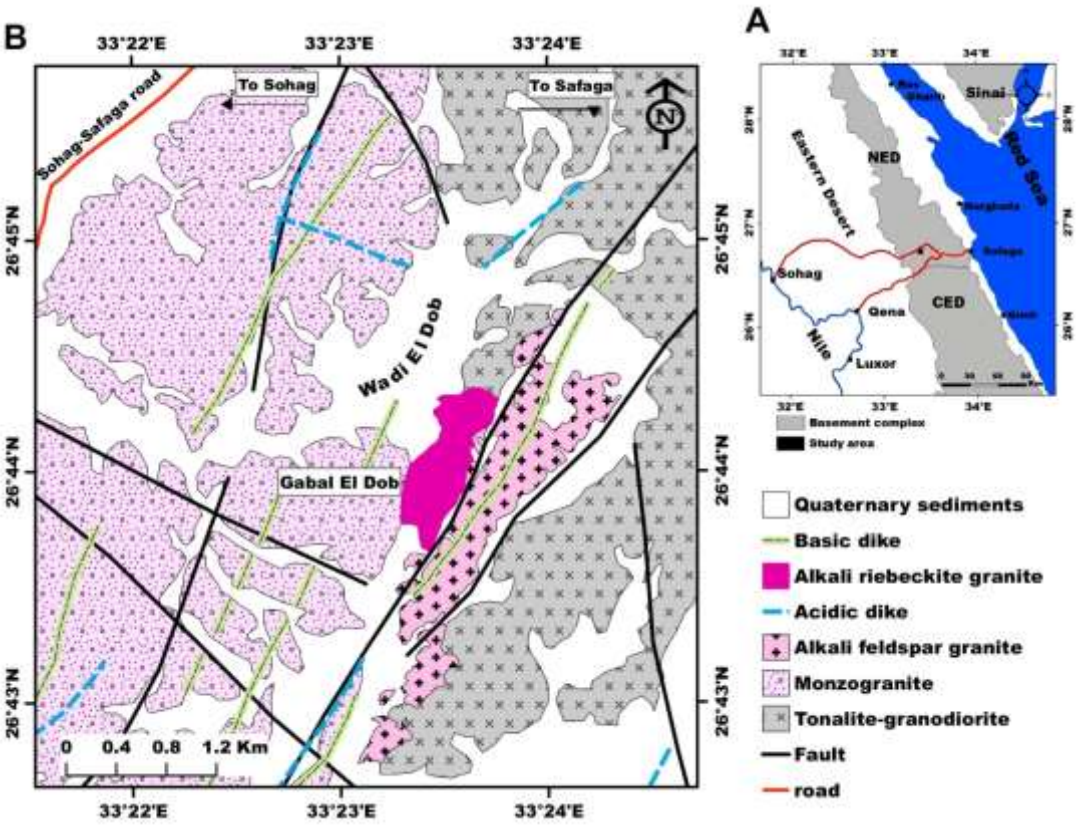

Fig. 1. (a) Location map of the investigated region, and (b) Geological map of Gabal El Dob area, northern Eastern Desert of Egypt.

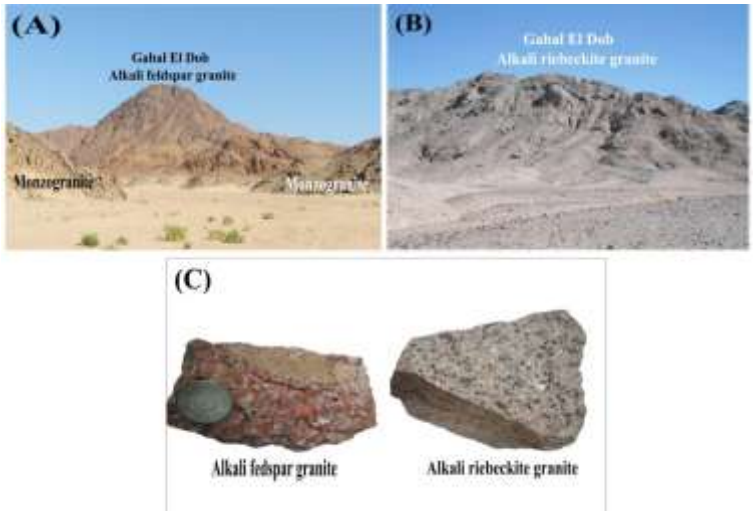

Fig. 2. (a) The alkali feldspar granite forms high elevated mountains surrounded by low hills of monzogranite, (b) Moderate outcrops of alkali riebeckite granite and (c) Contrast between the two granitic phases in hand specimen.

The alkali riebeckite granite forms a small elongated body located in the western vicinity of the alkali feldspar granite. It occurs as moderate to high mountains (Fig. 2b). This granite is medium-to coarse-grained, creamy to pale pink perthitic granite (Fig. 2c). Rb-Sr age of this granite indicates a Cambrian age of 522±21 Ma (Abdel Rahman, 2006). Thus, the investigated alkali riebeckite granite was emplaced following the termination of the Pan-African orogeny. Field observations indicate that this rock represents the youngest rock unit in the study area.

3. Materials and Methods

The methods employed in this study include geological mapping and sampling of the alkali feldspar and alkali riebeckite granites from Gabal El Dob area. About 24 fresh whole-rock samples were collected from rock exposures of the two granitic phases. Fresh samples were chosen with minimum alteration effects. The representative samples, comprising whole-rock granites were processed into thin sections for petrographic and mineralogic studies at the Nuclear Materials Authority, Egypt, while the chemical analyses of major, trace and rare earth elements were carried out using ICP-AES analytical methods at the Acme Analytical Laboratories, Vancouver, Canada.

4. Results

4.1 Petrography of the granites

Mineralogically, the alkali feldspar and alkali riebeckite granites of Gabal El Dob area can be differentiated into subsolvus and hypersolvus perthitic granites, respectively. The subsolvus granite is medium-grained and equigranular with hypidiomorphic texture. It is composed essentially of potash feldspar, quartz and plagioclase (Fig. 3a). The accessory minerals include biotite, muscovite, zircon, fluorite and iron oxides. Chlorite, sericite, epidote and calcite are the secondary minerals. Quartz found as large subhedral and anhedral fine-grained crystals. In some samples, it shows a graphic-like intergrowth texture with potash feldspar. Subhedral potash feldspar grains consist of string- and patch perthitic microcline and minor orthoclase (Fig. 3b). Plagioclase crystals are partly altered to sericite. Some crystals occur as inclusions in the large crystals of potash feldspar. Biotite is strongly pleochroic and slightly altered to chlorite (Fig. 3c). Zircon is characterized by zonation and inclusions of radioactive minerals.

The hypersolvus granite is medium-grained, composed of potash feldspar, quartz and alkali amphibole. Apatite, titanite, zircon, allanite, ilmenite and fluorite are accessories (Fig. 3d). Potash feldspar is mainly microcline-microperthite and less commonly orthoclase microperthite. It occurs as large subhedral crystals and shows a thin albite rim in some crystals. Feldspars are commonly sericitized. Alkali amphibole is ranging in compositions from arfvedsonite, to riebeckite rims (Fig. 3e). It occurs as subhedral prismatic crystals (Fig. 3f). In some instances, it is altered to chlorite. The alkali amphiboles are commonly twinned and large crystals usually contain zircon, allanite and iron oxides. Zircon is dominantly associated with quartz. Allanite is widespread and mostly enclosed in alkali amphiboles. Magnetite and ilmenite are the main opaque minerals and are associated with alkali amphiboles.

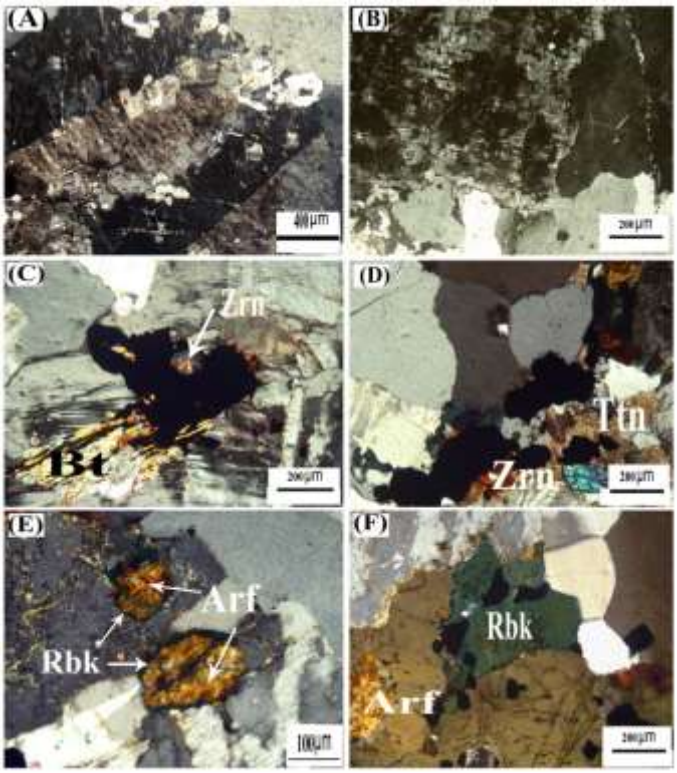

Fig. 3. Petrographic characteristics of Gabal El Dob subsolvus and hypersolvus granites, (a) Potash feldspar (orthoclase perthite) in the subsolvus granite, C.N., (b) Antiperthite in the subsolvus granite, C.N., (c) Biotite enclosing zircon with wide pleochroic halos in the subsolvus granite, C.N., (d) Quartz associates titanite and zircon in the hypersolvus granite, C.N., (e) Riebeckite rim as alteration of arfvedsonite, C.N., and (f) Subhedral crystals of riebeckite locally present interstitial between feldspars and quartz, C.N. Arf: arfvedsonite, Bt: Biotite, Rbk: riebeckite, Ttn: Titanite, Zrn: Zircon.

4.2 Geochemistry

4.2.1 Major and trace elements characteristics

The whole-rock chemical analyses of the studied subsolvus alkali feldspar granite and hypersolvus alkali riebeckite granite are listed in Table (1). Overall, the analysed granitic samples contain high SiO_2 (74.56–76.95 wt%) and K_2O (4.12–5.31 wt%) contents with high total alkalis (K_2O+Na_2O=8.0–9.8; Table 1). They fall in the field of alkali granite in the R_1-R_2 cationic classification diagram (Fig.4). Al_2O_3 contents vary between 11.85 and 12.62 wt%, exhibiting peralkaline nature for the hypersolvus granite and metaluminous to weakly peraluminous characteristics for the subsolvus granite (Fig. 5). CaO, MgO and P_2O_5 contents are very low (av. 0.43, 0.10, and 0.02, respectively). Contrastingly, the hypersolvus granite is higher in total alkalis, CaO, Ga, Zr, Nb, Y and ΣREE. Based on the classification of Frost et al. (2001), the two types of granite are mainly classified as ferroan and calc–alkalic to alkali-calcic (Fig. 6). The classification defines the A-type granitoids as a group of rocks comprising ferroan, alkaline to alkali-calcic.

The two granitic phases have high and variable contents of ΣREE, especially in the hypersolvus granite (Fig. 7a). The REE patterns are characterized by moderately fractionated LREE and nearly flat HREE patterns with pronounced negative Eu anomalies (Eu/Eu* = 0.18–0.35; Table 1). The high abundances of REE-bearing minerals in the hypersolvus granite interpret the presence of high values of ΣREE (av.= 530ppm; Table 1) in this rock relative to that of the subsolvus granite (av.= 121ppm; Table 1). All analysed samples have high concentrations of Rb, Th, U, Zr, Hf, Y and LREE and strong negative anomalies of Ba, Sr, Ti and P in the primitive mantle-normalized spidergrams (Fig. 7b). Nb/Ta ratios are gradually increase from the subsolvus granite (av.=10.54) to the hybersolvus granite (av.=16.83; Table 1). Negative Nb–Ta anomalies are observed in the subsolvus granite and Nb/La ratios are relatively constant over the whole samples ranging between 0.53 and 0.69 (Table 1).

Table 1. Major (wt.%) and trace elements (ppm) concentrations of Gabal El Dob A-type granites, northern Eastern Desert, Egypt.

Rock type	Subsolvus alkali feldspar granite						Hypersolvus alkali riebeckite granite					
Sample No.	POG -1	POG -2	POG -3	POG -4	POG -5	Av.	AOG -1	AOG -2	AOG -3	AOG -4	AOG -5	Av.
Major oxides (wt.%)												
SiO_2	76.92	75.83	77.28	76.95	77.08	76.81	75.22	76.64	74.56	75.77	74.84	75.41
TiO_2	0.15	0.17	0.12	0.21	0.14	0.16	0.25	0.19	0.28	0.21	0.26	0.24
Al_2O_3	11.91	12.26	11.85	11.97	12.14	12.03	12.62	12.12	12.37	12.46	12.48	12.41
Fe_2O_3	1.21	0.89	0.82	0.96	0.86	0.95	0.69	0.41	0.92	0.53	0.87	0.68
FeO	0.24	0.26	0.27	0.29	0.25	0.26	0.37	0.28	0.45	0.33	0.41	0.37
MnO	0.04	0.03	0.03	0.03	0.04	0.03	0.06	0.04	0.08	0.05	0.06	0.06
MgO	0.08	0.09	0.07	0.07	0.07	0.08	0.12	0.11	0.15	0.11	0.13	0.12
CaO	0.39	0.35	0.33	0.38	0.36	0.36	0.38	0.45	0.85	0.37	0.45	0.50
Na_2O	3.96	4.57	4.18	4.12	4.12	4.19	4.97	4.52	4.87	4.92	4.49	4.75
K_2O	4.15	4.45	4.12	4.25	3.89	4.17	4.82	4.92	4.69	4.88	5.31	4.92
P_2O_5	0.01	0.02	0.01	0.01	0.02	0.01	0.02	0.01	0.02	0.02	0.02	0.02
L.O.I	0.94	1.08	0.92	0.76	1.03		0.48	0.31	0.76	0.35	0.68	
Total %	100	100	100	100	100		100	100	100	100	100	
AI	0.92	1.01	0.96	0.95	0.91	0.95	1.01	1.05	1.02	1.07	1.05	1.04
Trace elements (ppm)												
Ba	133	236	126	105	187	157	96	85	116	92	106	99
Rb	127	167	120	75	145	126	77	72	121	76	81	85
Sr	29	56	24	19	43	34	23	21	36	21	28	25.8
Ga	19.5	22.4	19.2	17.2	20.1	19.7	31	25	36	28	32	30.4
Ta	1.29	1.47	1.26	1.05	1.36	1.29	3.9	3.6	4.8	3.8	4.1	4.04
Nb	13.5	15.9	12.8	11.9	13.8	13.6	68	61	75	65	71	68
Hf	5.67	7.24	5.46	5.46	6.41	6.05	9.6	9.5	13.8	9.2	10.8	10.5
Zr	143	162	131	127	148	142	560	472	689	486	562	553
Y	30	39	27	26	33	31	51	46	68	48	61	54.8
Pb	80	134	73	59	89	87	39	21	46	28	41	35
Zn	192	298	168	168	221	209	83	64	109	77	85	83
Th	16.5	15.4	19.5	21.6	15.8	17.8	33.7	28.2	27.9	31.9	29.6	30.3
U	9.4	7.8	10.5	10.7	8.4	9.3	5.1	6.8	4.9	6.4	5.6	5.8
Th/U	1.76	1.99	1.86	2.02	1.88	1.90	6.61	4.15	5.69	4.98	5.29	5.25
Nb/La	0.54	0.57	0.61	0.6	0.53	0.57	0.58	0.69	0.53	0.61	0.58	0.59
Nb/Ta	10.47	10.82	10.16	11.33	10.15	10.54	17.44	16.94	15.63	17.11	17.32	16.83
10000*Ga /Al	2.71	3.06	3.09	3.13	3.45	3.08	3.90	4.24	4.64	4.84	5.50	4.62
REE (ppm)												
La	25	28	21	20	26	24	118	88	141	107	123	115.4
Ce	50	64	38	47	55	50.8	221	197	254	207	241	224
Pr	5	7.6	4.9	3.9	5.1	5.3	26.61	21.9	32.52	25.74	27.35	26.82
Nd	10	25	16	11	13	15	102	84	123	97	109	103
Sm	2.62	4.83	3.78	1.36	4.93	3.5	19.49	11.87	25.56	15.13	21.42	18.69
Eu	0.23	0.42	0.21	0.1	0.31	0.25	1.72	1.14	1.79	1.56	1.59	1.56
Gd	4.3	3.25	3.25	1.26	2.31	2.87	14.93	10.59	16.49	12.16	15.88	14.01
Tb	1.36	0.63	0.84	0.21	0.52	0.71	1.8	1.33	2.24	1.53	2.07	1.79
Dy	4.62	4.41	7.14	1.26	5.77	4.64	10.18	7.72	13.46	8.48	12.84	10.54
Ho	1.68	0.84	1.89	0.84	1.26	1.3	1.87	1.54	2.41	1.57	2.14	1.91
Er	5.67	3.15	7.24	1.36	4.72	4.43	5.21	3.97	6.19	4.46	5.9	5.15
Tm	1.36	0.735	1.47	0.84	1.26	1.13	0.76	0.73	0.93	0.67	0.94	0.81
Yb	6.51	5.56	10.29	2.73	5.88	6.19	5.26	3.98	6.39	4.62	6.47	5.34
Lu	0.84	0.84	1.575	0.42	1.26	0.99	0.87	0.83	1.03	0.79	1.07	0.92
ΣREE	119	149	117	92	127	121	529	434	627	487	570	530
Normalized ratios (Anders and Grevesse, 1989)												
Eu/Eu*	0.21	0.32	0.18	0.23	0.28	0.24	0.31	0.31	0.26	0.35	0.26	0.23

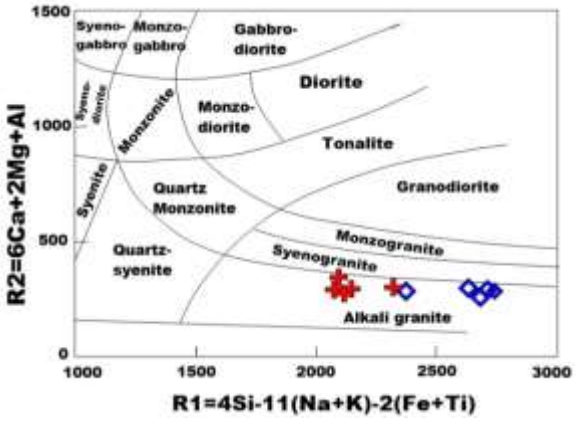

Fig. 4. R_1-R_2 classification diagram of Gabal El Dob granites (after De La Roche et al. (1980) ◇: Subsolvus alkali feldspar granite, ✚: Hypersolvus alkali riebeckite granite.

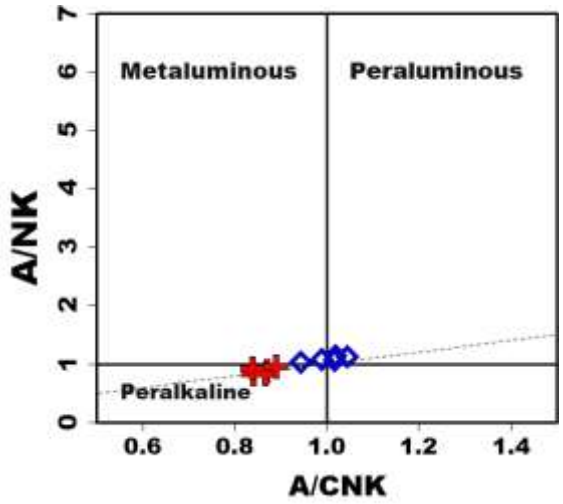

Fig. 5. ANK vs. A/CNK plot of Gabal El Dob granites (after Maniar and Piccoli, 1989). Symbols are the same as in Fig. 4.

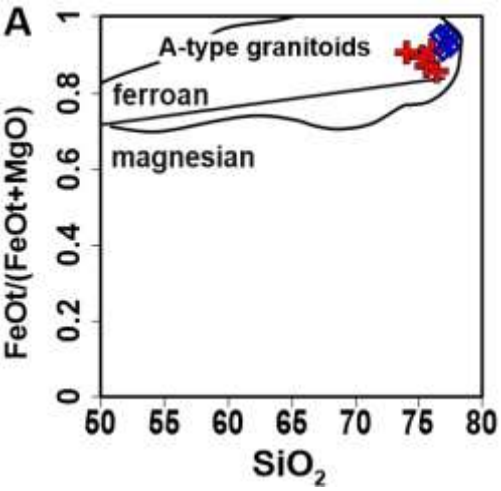

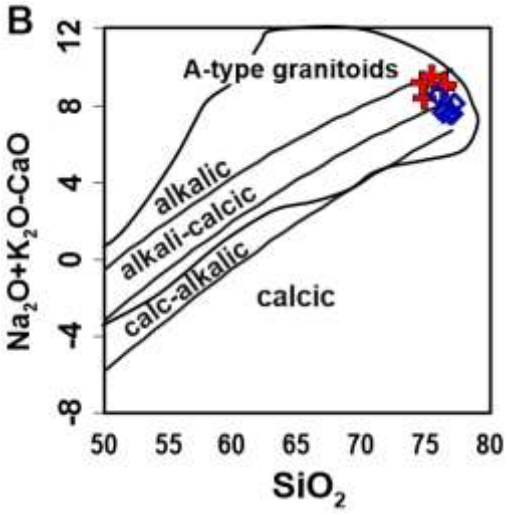

Fig .6. (a) FeOt/(FeOt+MgO) and (b) Na_2O+K_2O-CaO vs. SiO_2 classification diagram (after Frost et al., 2001). Symbols are the same as in Fig. 4.

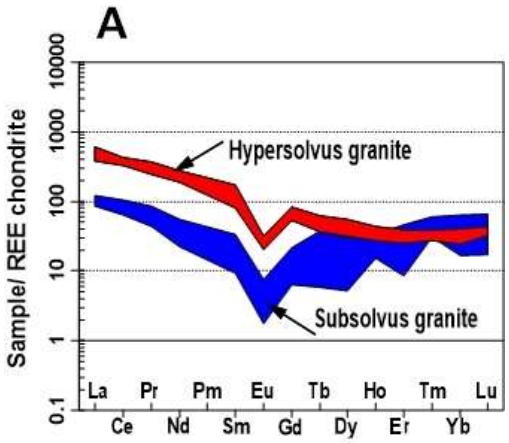

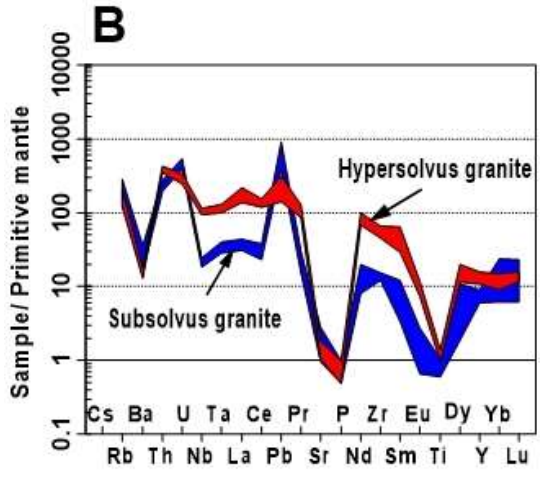

Fig. 7. (a) Chondrite-normalized REE patterns and (b) Primitive mantle-normalized trace element spidergrams of Gabal El Dob granites. Chondrite and PM normalization factors from McDonough and Sun (1995), and Anders and Grevesse, 1989, respectively.

5. Discussion

5.1 Genetic type

The studied granitic phases of Gabal El Dob show similarities to A-type granitoids, especially the hypersolvus granite, in their field and mineralogical characteristics. The presence of alkali arfvedsonite and riebeckite in the hypersolvus granite indicated that this granite share common features with the A-type granites (Bonin, 2007; Collins et al., 1982). However, the subsolvus granite is free of mafic alkaline minerals. The mean values of 10,000*Ga/Al along the analysed samples are 3.08 and 4.62 for the subsolvus and hypersolvus granites, respectively, the equivalent ratio suggested for A-type granites is 3.75 (Whalen et al., 1987). In the discrimination diagrams K_2O+Na_2O, FeOt/MgO, Nb and Zr vs. 10000*Ga/Al (Fig. 8a-d), the studied granitic samples plot within the A-type granite field of Whalen et al. (1987). Moreover, in FeOt/MgO and $(K_2O+Na_2O)/CaO$ vs. (Zr+Nb+Ce+Y) diagrams (Fig. 8e&f), the subsolvus granite fall in the field of fractionated I-type and the hypersolvus granitic samples are plotted in the A-type granite field. It is concluded that the subsolvus granite has a transitional characters between fractionated I-type and A-type granitoids, but the hypersolvus granite has most characteristics of A-type granites.

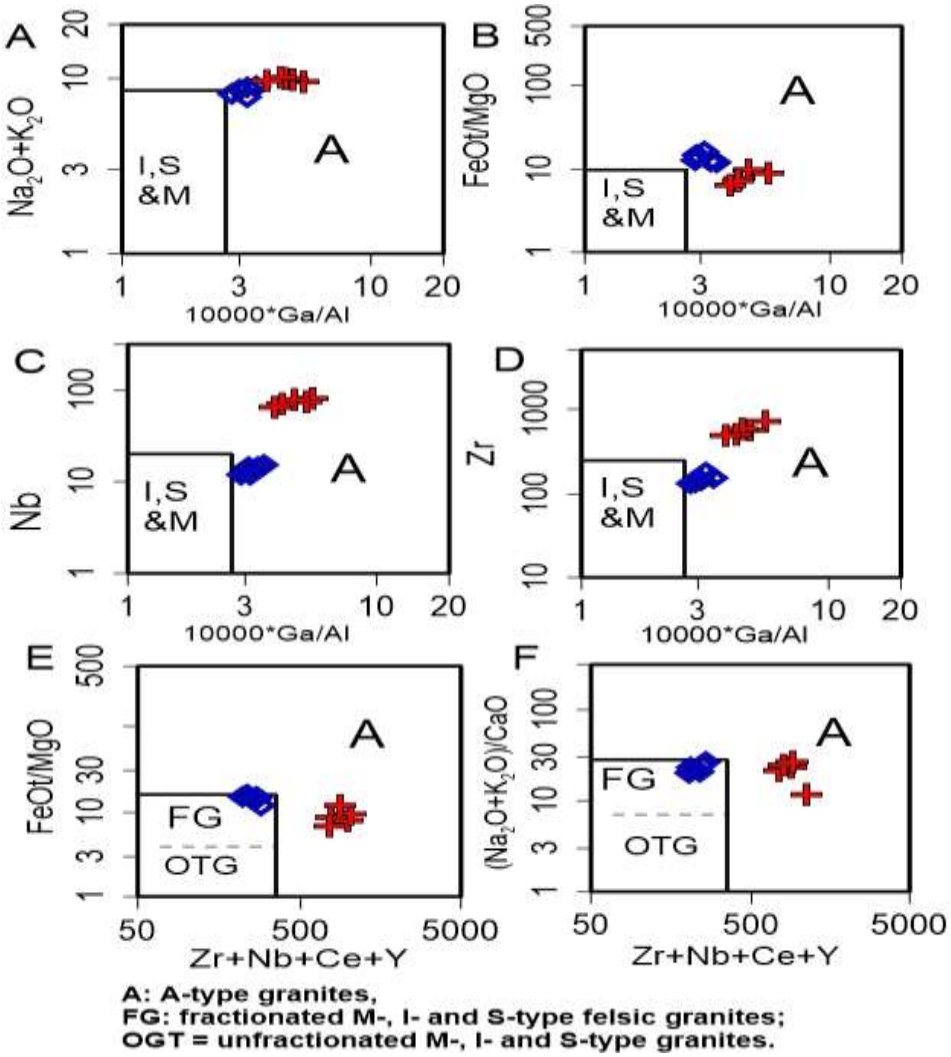

Fig. 8. (a) Na_2O+K_2O, (b) FeOt/MgO, (c) Nb, (d) Zr vs. 10000*Ga/Al and (e) FeOt/MgO, (f) $(Na_2O+K_2O)/CaO$ vs. (Zr+Nb+Ce+Y) classification diagrams (Whalen et al., 1987).

5.2 Tectonic setting

The tectonic setting of the two granitic types of Gabal El Dob can be evaluated on the basis of trace element geochemistry. The analysed samples are plotted on the Rb vs. (Y + Nb) diagram of Pearce et al. (1984) whereas the subsolvus granite is located in the field of the post-collisional tectonic setting delineated by Pearce (1996) and the hypersolvus granite is plotting in the within plate setting (Fig. 9a). In addition, all analysed granitic samples are falling in the A-type field proposed by Whalen et al. (1987). Furthermore, on the Nb vs. Y discrimination diagram (Fig. 9b) the subsolvus granite is located at the boundary between the volcanic arc and within plate fields, but the hypersolvus granite is falling in the within plate tectonic setting. All samples plot in the field of A-type granites related to the Arabian Nubian Shield (ANS) defined by Stern and Gottfried (1989).

In the Nb-Y-3Ga ternary plot and Rb/Nb–Y/Nb discrimination diagram of Eby (1992), the subsolvus granite plot into the A_2 group (Fig. 10a,b), which supports the post-orogenic nature of this granite type. On the other hand, the hypersolvus granite is located in the A_1 filed indicated anorogenic setting for this type of granite.

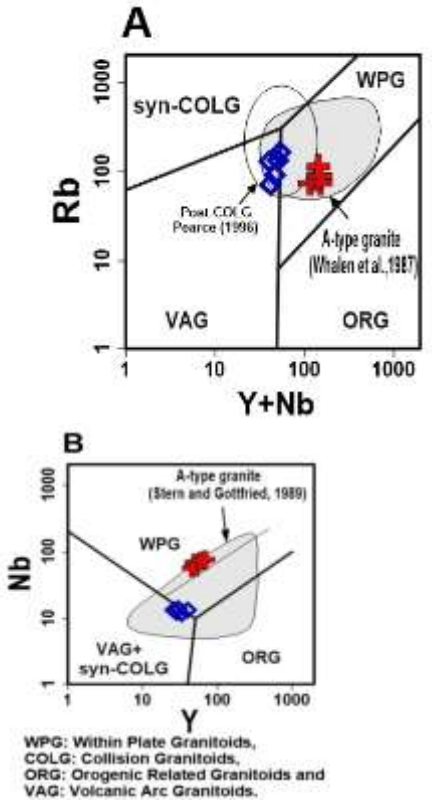

Fig. 9. (a) Rb vs. (Y+ Nb) and (b) Nb vs. Y tectonic discrimination diagrams of Gabal El Dob A-type granites after Pearce et al. (1984). Symbols are the same as in Fig. 4.

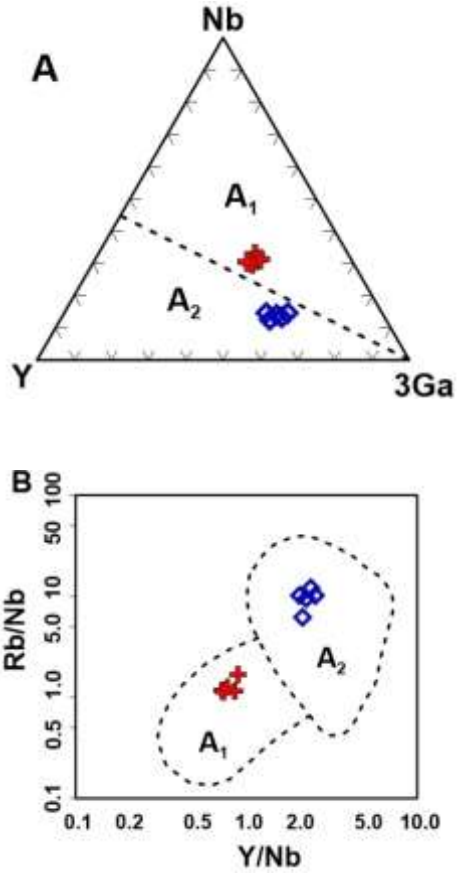

Fig.10. Plots of Gabal El Dob granites in Nb-Y-3Ga ternary diagram and Y/Nb vs. Rb/Nb plot (after Eby, 1992). Symbols are the same as in Fig. 4.

5. 3 Rare metal exploration

The ground radiometric survey upon the two granitic types of Gabal El Dob don not shows local enrichment of U and Th mineralization. Generally, the occurrence of these mineralizations is usually depending on the effect of the hydrothermal reworking upon the rock. The hydrothermal overprint is very lack in the study area and, if present it is attributed to surficial weathering. However, the hypersolvus alkali riebeckite granite of Gabal El Dob is enriched in Zr and REE compared to the subsolvus alkali feldspar granite. The agpaitic index (AI= atomic ratio of Na+K/Al) is higher in the hypersolvus granite (av. 1.04) than in the subsolvus granite (av. 0.95) indicated that Zr is increased with increasing the alkalinity of the rock (Watson, 1979). The high values of Zr and ΣREE in the hypersolvus granite are interpreted to the extreme abundance of zircon and allanite in this granite. They are associated together within larger crystals, generally alkali amphibole (Fig. 11a). The elemental mapping upon this association of allanite and zircon indicated high contents of LREE

and Zr besides the major components of the alkali amphibole (Si, Al, Fe, Na and K; Fig. 11b). SEM image and EDX analysis of individual grains of allanite revealed a clear predominance of LREE in this mineral (highs up 50%; Fig. 12).

The mean U and Th abundances (9.3ppm and17.8ppm, respectively) of the subsolvus granite are higher than to those suggested for granitic rocks (3 ppm, 10 ppm; Taylor, 1966). With increased alkalinity in the hypersolvus granite, the mean U content decreases to 5.8ppm and the mean Th values rises to 30.3ppm. As a result, the mean Th/U ratios changes from 1.90 in the subsolvus granite to 5.25 in the hypersolvus granite (Table 1). The high abundances of REE and Zr in hypersolvus granite along with the elevated background values of U and Th in both granitic phases could be used as an indicator for rare-metal exploration in Gabal El Dob area.

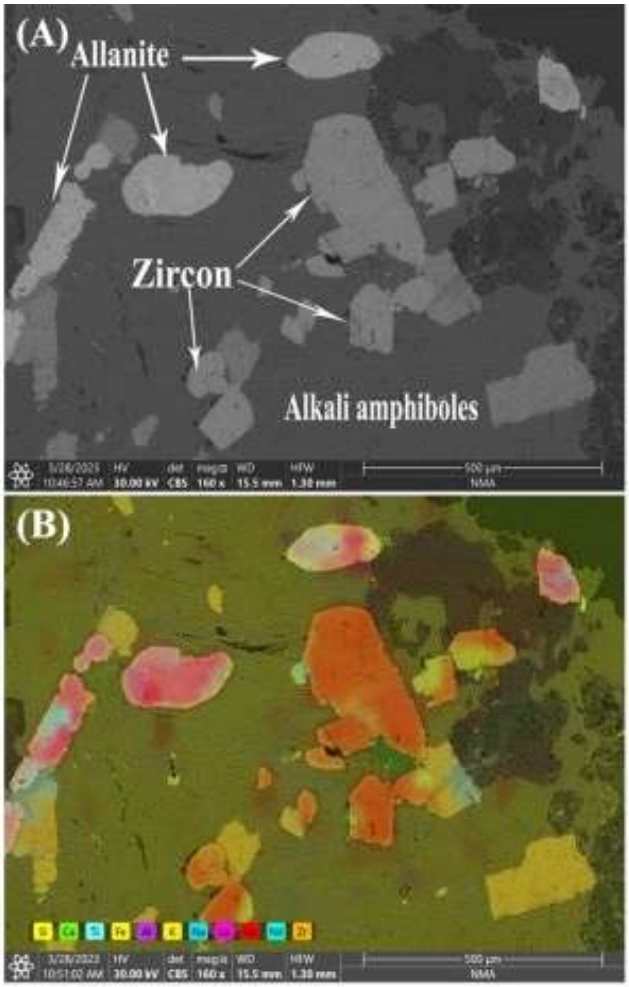

Fig. 11. Distribution of zircon and allanite in the hypersolvus granite of Gabal El Dob, (a) SEM image showing association of allanite and zircon enclosed within alkali amphiboles, and (b) Elemental mapping of the same photo describes the distribution of REE and Zr in their bearing minerals.

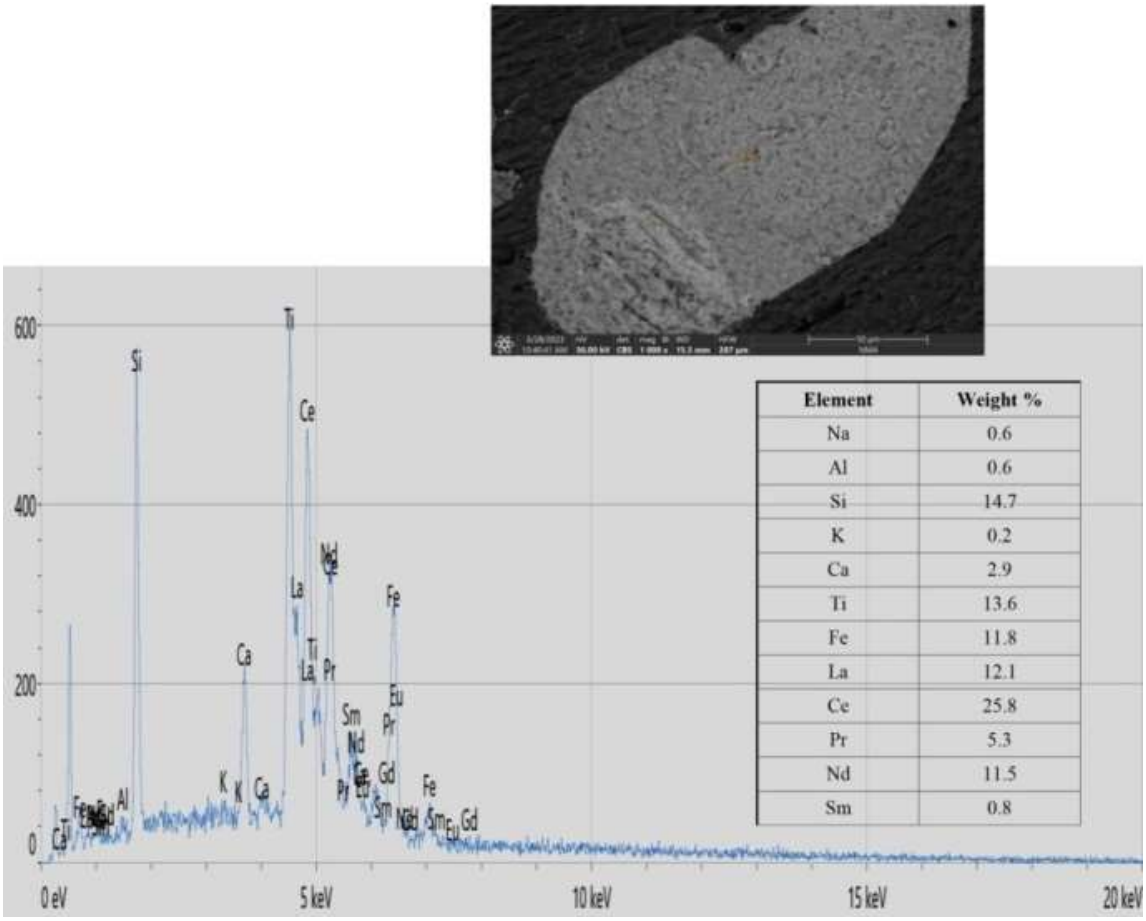

Fig. 12. SEM image and EDS analysis of allanite indicated this mineral is the main carrier of REE in the hypersolvus granite.

6. Conclusions

In the present study, the post-tectonic granites of Gabal El Dob area are classified petrographically into subsolvus and hypersolvus granites. The two granitic types composed essentially of perthites and quartz with little amount of plagioclase. The accessory minerals show variations along the two granitic phases. The hybersolvus granite contains alkali amphiboles represented by arfvedsonite and riebeckite and enriched with allanite and zircon.

The studied granitic phases show different chemical composition and tectonic setting implying that they are genetically unrelated and may have been derived from different sources. The subsolvus granite is metaluminous to slightly peraluminous, fractionated I-type granite with affinity to A-type granitoids formed in post-orogenic environment. The hypersolvus granite is peralkaline in nature and belongs to anorogenic A-type granitoids. The hypersolvus granite has higher contents of Zr, Nb and REE relative to the subsolvus granite but relatively lower contents of U and Th.

Mineralogical studies indicated that the high concentrations of Zr (av. 553ppm) and ΣREE (av. 530) in the hypersolvus granite are connected with the high abundances of zircon and allanite. These elevated contents along with the high background values of U and Th in both granitic phases could be used as an indicator for rare-metal exploration in Gabal El Dob area.

References

Abdel-Rahman, A.M. (2006) Petrogenesis of anorogenic peralkaline granitic complexes from eastern Egypt. *Mineral. Mag.*, **70**, 27–50.

Abdel-Rahman, A.M. and Martin, R.F. (1990) The Mount Gharib A-type granite, Nubian Shield: petrogenesis and role of metasomatism at the source. *Contrib. Mineral. Petrol.*, **104**, 173–183.

Anders, E. and Grevesse, N. (1989) Abundances of the elements: meteoritic and solar. *Geochim. Cosmochim.* **53**, 197–214.

Bentor, Y.K. (1985) The crustal evolution of the Arabo–Nubian Massif with special reference to the Sinai Peninsula. *Precamb. Res.*, **28**, 1–74.

Bonin, B. (2007) A-type granites and related rocks: evolution of a concept, problems and prospects. *Lithos*, **97**, 1–29.

Collins, W.J., Beams, S.D., White, A.J.R. and Chappell, B.W. (1982) Nature and origin of A-type granites with particular reference to south eastern Australia. *Contrib. Mineral. Petrol.*, **80**, 189–200.

De La Roche, H., Leterrier, J., Grand Claude, P. and Marchal, M. (1980) A classification of volcanic and plutonic rocks using R_1-R_2 diagrams and major element analyses - its relationships with current nomenclature. *Chem. Geol.*, **29**, 183-210.

Eby, G. N. (1992) Chemical subdivision of the A-type granitoids: petrogenetic and tectonic implications. *Geology*, **20**, 641– 644.

El-Naggar, I., Hassaan, M., Shahin, T., Omar, S. and Khalil, A. (2022) Geochemical exploration of U-Mo-W younger late-orogenic granites, El-Urf - El Dob - Abu-Kharif geochemical province, Safaga-Qena tectonic discontinuity belt, Eastern Desert, Egypt. *Al-Azhar Bulletin of Science*, **33**, 145-157.

El-Sayed, M.M., Furnes, H., Obeid, M.A. and Hassanen, M.A. (2001) The Mueilha intrusion, Eastern Desert, Egypt: a postorogenic, peraluminous, rare-metal bearing granite. *Chem. Erde.*, **61**, 294–316.

Farahat, E., Mohamed, H., Ahmed, A. and El Mahallawi, M. (2007) Origin of I-and A-type granitoids from the Eastern Desert of Egypt: implications for crustal growth in the northern Arabian–Nubian Shield. *J. Afr. Earth Sc.*, **49**, 43–58.

Frost, B.R., Barnes, C.G., Collins, W.J., Arculus, R.J., Ellis, D.J. and Frost, C.D. (2001) A Geochemical Classification for Granitic Rocks. *J. Petrol.*, **42**, 2033-2048.

Hammed, M., Shallaly, N., Abdel Ghani, M., Badr, Y. and Sayed, S. (2020) Application of remotely sensing data in the geologic and radioactive mapping of Wadi Fatirah Precambrian rocks, North Eastern Desert, Egypt. *Nucl. Sci. Sci. J.*, **9**, 227- 253.

Harris, N.B.W. (1982) The petrogenesis of alkaline intrusives from Arabia and northeast Africa and their implications for within plate magmatism. *Tectonophysics*, **83**, 242–258.

Hashad, A.H. (1980) Present status of geochronological data on the Egyptian basement complex. In: Cooray PG, Tahoun SA (eds) Evolution and mineralization of the Arabian–Nubian Shield. Inst. Appl. Geol. Jeddah Bull, **3**. Pergamon, Oxford, pp 31–46.

Hassanen, M.A. and Harraz, H.Z. (1996) Geochemistry, Sr- and Nd isotopic study on the rare-metals bearing granitic rocks, Central Eastern Desert, Egypt. *Precamb. Res.*, **80**, 1–22.

Katzir, Y., Eyal, M., Litvinovsky, B.A., Jahn, B.M., Zanvilevich, A.N., Valley, J.W., Beeri, Y., Pelly, I. and Shimshilashvili, E. (2007) Petrogenesis of A-type granites and origin of vertical zoning in the Katherina pluton, Gebel Mussa (Mt. Moses) area, Sinai, Egypt. *Lithos*, **95**, 208–228.

Maniar, P. D. and Piccoli, P. M., (1989) Tectonic discrimination of granitoids. Geol. Soc. Am. Bull., 101: 635-643.

Marks, M., Vennemann, T., Siebel, W. and Markl, G. (2003) Quantification of magmatic and hydrothermal processes in a peralkaline syenite–alkali granite complex based on textures, phase equilibria, and stable and radiogenic isotopes. *J. Petrol.*, **44**, 1247-1280.

McDonough, W.F. and Sun, S. (1995) The composition of the Earth. *Chem. Geol.*, **120**, 223-253.

Moghazi, A.M. (1999) Magma source and evolution of late Neoproterozoic granitoids in the Gabal El Urf area, Eastern Desert, Egypt: geochemical and Sr–Nd isotopic constrains. *Geol. Mag.*, **136**, 285–300.

Moussa, E.M., Stern, R.J., Manton, W.I. and Ali, K.A. (2008) SHRIMP zircon dating and Sm/Nd isotopic investigations of Neoproterozoic granitoids, Eastern Desert, Egypt. *Precamb. Res.*, **160**, 341–356 (2008).

Pearce, J. A. (1996) Sources and settings of granitic rocks. Episodes, **19**, 120–125.

Pearce, J.A., Harris, N.B.W. and Tindle, A.G. (1984) Trace element discrimination diagrams for the tectonic interpretation of granitic rocks. *J. Petrol.*, **25**, 959–983.

Rogers, J.J.W., Ghuma, M.A., Nagy, R.M., Greenberg, J.K. and Fullgar, P.D. (1978) Plutonism in Pan-African belts and the geologic evolution of northeastern Africa. *Earth Planet. Sci. Lett.*, **39**, 109–117.

Shahin, T.M. (2015) Geology, geochemistry and petrotectonicof the basement rocks at Gebel El Dob area, North Eastern desert, Egypt. Unpublished Ph. D. thesis, Faculty of Science, Al-Azhar University.

Stern, R. J. and Gottfried, D. (1989) Discussion of the paper "Late Pan-African magmatism and crustal development in northeastern Egypt". *Geol. J.*, **24**, 371–374.

Taylor, S.R. (1966) The application of trace element data to problems in petrology; Physics and Chemistry of the Earth, **6**, 135-213.

Watson, E.B. (1979) Zircon saturation in felsic liquids: experimental results and applications to trace element geochemistry. *Contrib. Mineral. Petrol*., **70**, 407–419.

Whalen, J. B., Currie, K. L. and Chappell, B. W. (1987) A-type granites: geochemical characteristics, discrimination and petrogenesis. *Contrib. Mineral. Petrol.*, **95**, 407–419.

Xie, L., Wang, R.C., Wang, D.Z. and Qiu, J.S. (2006) A survey of accessory mineral assemblages in peralkaline and more aluminous A-type granites of the southeast coastal area of China. *Mineral. Mag.*, **70**, 709-729.

الخصائص الجيوكيميائية واستكشاف المعادن النادرة لجرانيتات جبل الدب من نوع (A-type)، الصحراء الشرقية، مصر

عمرو عبدالعاطى عبدالحميد

هيئة المواد النووية- ص.ب ٥٣٠ المعادى، القاهرة، جمهورية مصر العربية

تقع منطقة جبل الدب في شمال الصحراء الشرقية المصرية، شمال غرب مدينة سفاجا على طريق سفاجا–سوهاج. تغطي هذه المنطقة بصخور القاعدة والتي تتكون من صخور الجرانيت القديمة وصخور الجرانيت الحديث. تتمثل صخور الجرانيت الحديث في وجود صخور جرانيت الفلسبار القلوى. توجد صخور جرانيت الفلسبار القلوى، وهى محور الدراسة، على هيئة أجسام ممدودة فى اتجاه شمال شرق. تم تقسيم هذه الصخور حسب الدراسات البتروجرافية والجيوكيميائية إلى جرانيت قلوى من نوع post–orogenic subsolvus وجرانيت قلوى من نوع anorogenic hybersolvus. تتشابه المعادن الاساسية فى هذين النوعين من الجرانيت فى وجود البيرثيت والكوارتز والبلاجيوكليز. أما المعادن الشحيحة فتختلف في كميتها وأنواعها، حيث يحتوي الأخير على معادن الأمفيبول القلوية بالإضافة إلى أنه يحتوى على نسبة عالية من معادن الزركون والالانيت. تؤكد الدراسة الجيوكيميائية لهذه الجرانيتات القلوية من نوع (A–type) على أنهم بهم نسب عالية من السيليكا وعناصر الصوديوم والبوتاسيوم، وبهم نسب قليلة من عناصر الماغنسيوم والكالسيوم والتيتانيوم. على الرغم من أن كلا النوعي يبدوان متجانسين نسبيًا من حيث وجود معظم العناصر الرئيسة والشحيحة، إلا أنهما يختلفان في أن الجرانيت من نوع anorogenic به نسب أعلى من عناصر التيتانيوم والحديد والجاليوم والزركونيوم والعناصر الارضية النادرة، ويحتوى على نسب اقل من عناصر الباريوم و الروبيديوم. تم تفسير وجود تركيزات عالية من العناصر الأرضية النادرة فى هذا الجرانيت بسبب وجود نسب عالية من معدن الالانيت الحامل لهذه العناصر. حيث يزداد وجود معدنى الألانيت والزركون تدريجياً بزيادة قلوية الصخر. يمكن استخدام التركيزات العالية للعناصر الارضية النادرة وعنصر الزركونيوم بالاضافة إلى ارتفاع الخلفية الاشعاعية المتمثلة فى ارتفاع تركيزات عنصرى اليورانيوم والثوريوم فى صخور الجرانيت الفلسبار القلوى كدلائل لزيادة التنقيب على العناصر النادرة في منطقة جبل الدب فى هذه الصخور.